Numerical models for the analysis of shear walls in light steel residential buildings

Nadia Baldassino, Riccardo Zandonini, Marco Zordan

Correspondence

Dr. Eng. Nadia Baldassino
Dept. Civil, Environmental and Mechanical Engineering
University of Trento
via Mesiano, 77
38123 Trento (IT)
Email: nadia.baldassino@unitn.it

Abstract

In recent years, the use of steel light housing structural solutions made of cold-formed thin-walled profiles (CFS) is becoming increasingly popular. Lightness, high structural efficiency, durability, rapidity and simplicity of erection of the building and its finishes are some of the main advantages of these systems, which make them attractive and competitive with respect to more traditional constructional solutions. In these buildings, which do have a skeleton made of cold-formed steel profiles completed by sheathings made of various materials, the key role of transmission of both vertical and horizontal loads from the floors to the foundation, is played by the shear walls. Recently, the University of Trento carried out a project aimed to develop an industrialized housing system made of CFS members. In this framework, experimental and numerical studies of the in-plane lateral response of shear walls were performed. In particular, this paper summarizes first the experimental program and then it focuses on the main features of numerical models and on their validation in both monotonic and cyclic regime. The critical parameters governing the response of these complex systems are finally identified and discussed.

Keywords

Lightweight steel residential buildings, Cold-formed thin-walled profiles, Shear Walls, In plane lateral response, Experimental study, Numerical modelling.

1 Introduction

With the aim to develop building systems able to support significant seismic events, in the last years, a new concept of residential steel building became popular. These buildings do have a skeleton made of cold-formed steel members finished with sheathings made of steel, or OSB panels, or gypsum fibre boards. Light weight, high structural efficiency, durability, rapidity and simplicity of installation of the building finishes are the main advantages of these new building systems, which have shown to be competitive with respect to the more traditional constructional ones. In addition, the lightness of these structures results in a significant benefit in terms of seismic performance, since horizontal forces are primarily related to the structural mass. Although the magnitude of these horizontal forces is relatively low, for a safe design the loading path through the building have to be clearly identified. In these buildings, the shear walls are key structural components for the seismic performance providing the bracing system and allowing the force transfer from the floors to the foundation. Several studies of these elements have already performed in several countries such as in Canada with Al-Kharat et al. [1,2] and DaBreo et al. [3] that highlighted the inelastic performance given by steel wall straps, and in USA where Buonopane et al. [4] and Liu et al. [5] carried out studies of the contribution of the sheathing to the wall performance. Similarly, Lu [6] and Chen [7] studied the influence of gypsum and wood panels on the lateral

response of cold-formed steel framed shear walls. In a wider framework, Padilla-Llano et al. [8] and also Schafer et al. [9] investigated the seismic performance of CFS framed buildings making particular attention to the numerical simulation of the shear walls. In Italy, few years ago, the University of Trento started a project aimed to develop an industrialized housing system made of CFS members. In this framework, an experimental and numerical study of the in-plane lateral response of shear walls was performed. The experimental programme, which comprises of monotonic and cyclic tests, considered several wall configurations differing from the type of bracing system and the possible presence of sheathing. The experimental tests enabled the calibration and validation of numerical models. In this paper, the main features of the experimental programme on the shear walls are summarized and the main findings discussed. The numerical models are then presented and discussed for three wall configurations: one unsheathed and two sheathed. Focus is on the main aspects that govern the simulation of these complex systems.

2 The experimental program

The experimental program, aimed to characterize the lateral response of the CFS shear walls, comprised a series of 21 specimens covering 16 different configurations. All the specimens had equal dimensions: 2400 mm of width and 3018 mm of height to simulate a typical single storey. As an additional feature, the steel framework is made using only one type of C section, either 100 mm or 150 mm

deep and 1.2 mm thick. The nominal steel yielding resistance was equal to 280 MPa. The 16 configurations differed in the type of bracing system, the presence of the hold-downs, the member depth, the spacing between the studs, the presence of the sheathing and eventually the type of sheathing. In particular, a total of 9 bracing systems were investigated including trussed bracing and diagonal straps bracing as depicted in Figure 1.
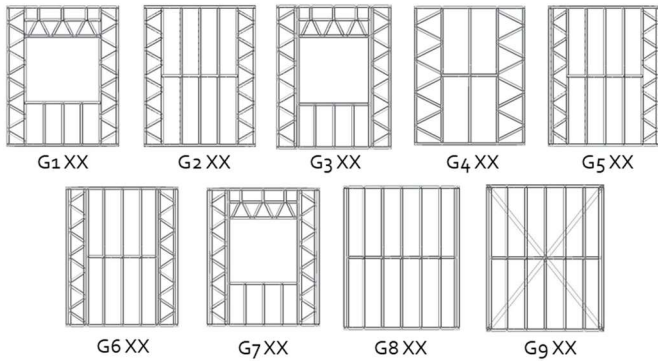

Figure 1 Bracing systems considered in the experimental program

All these aspects are reflected in the nomenclature reported in Figure 2; in Table 1 a concise description of all bracing systems is provided.
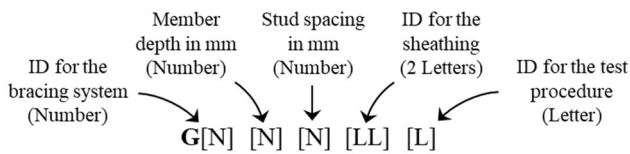

Figure 2 Nomenclature of the shear wall's specimens

Table 1   Bracing system description

Bracing System ID	Structural system
G1	Trussed frame with window opening and hold-downs on both chords
G2*	Trussed frame without hold-downs
G2	Trussed frame with hold-downs on outer chords
G3	Trussed frame with window opening, double inner chord and hold-downs on outer chords
G4	Trussed frame and hold-downs on outer chords
G5	Trussed frame with double outer chords, and hold-downs on external chords
G6	Trussed frame with double inner & outer chords and hold-downs on outer chords
G7	Trussed frame with double outer and inner chords, with window opening and hold-downs on external chords
G8	No bracing system. This configuration is only tested with skin
G9	Diagonal straps with double outer chords and hold-downs on external chords

Five wall configurations have sheathing on both sides in order to investigate how the contribution of the skin affects the global response of the wall. Two panels for wall side were attached to the

steel frame using 4,2 mm x 25 mm self-drilling screws. Five different panel's material were considered: four different types of cement board and one gypsum board. Table 2 reports the ID, the material type and the thickness adopted for the panels. The sheathed walls are characterized by two different types of sheathing, one per side, identified by two letters depending on the sheathing ID. For example, the G9 100 400 GH configuration has the G9 bracing system built using 100 mm deep members, studs' spacing equal to 400 mm and sheathed with G panels on one side and H panels on the other side. On the contrary, the unsheathed configurations are identified with the XX letters.

Table 2   Type of sheathings

ID	Sheathing Material	Nominal thickness [mm]
B	Fibreboard which combines Gyproc & cellulose fibres	12,5
E	Cement board reinforced with fibre	10,0
F*	Wood-fibre cement sheet	12,5
G	Cement-bonded panels reinforced with a glass fibre mesh	12,5
H	Gypsum fibreboard	12,5

2.1   The test set-up and the loading procedure

Being the goal of the project to characterize the lateral behaviour of the walls for a building under service loads, the specimens were subjected first to a vertical load, simulating the service state, and then to a horizontal displacement. An ad-hoc test set-up was used. The vertical load was applied on the top of the walls along the whole length and was equal to 17,07 kN/m, while the horizontal displacement was applied at the top of the wall using an MTS actuator. The horizontal displacement followed either a monotonic or a cyclic protocol according to the ECCS recommendations (ECCS, 1986 [10]). In detail, the ECCS protocol recommends to evaluate a conventional yielding displacement (e_y) based on the monotonic test result, and to use it to define the amplitude of the cycles (Figure 3).
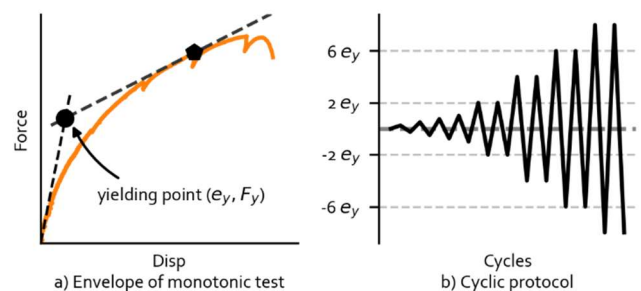

Figure 3 The cyclic procedure according to the ECCS recommendations [10]

2.2   The test results

Herein are briefly summarized the main results of the experimental program. Detailed information can be found in [11] and [12]. Table 3 and Table 4 report the results in terms of resistance and stiffness of the unsheathed and sheathed configurations, respectively. The stiffness is evaluated as the secant stiffness at the 40% level of the maximum strength in accordance with AISI S907-2013 [13]. As to the unsheathed specimens, Figure 4a) shows the comparison, in terms

of force-displacement curves, of all the G2 configurations. The curves make apparent the significant increase of resistance that the hold downs provide to the system. On the contrary, the influence of the depth of the member's section is rather limited. Indeed, the blue curves show the responses of the configurations with 150 mm depth members while the orange curves show the responses of the ones with 100 mm depth members. Figure 4b) shows the force displacement curves of the configurations characterised by the trussed bracing systems, including the ones with the windows opening (G1, G2, G3, G5 and G6).

Table 3   Monotonic test results: unsheathed configurations

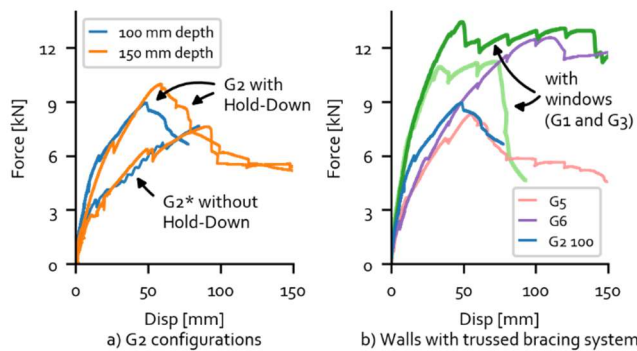| Specimen ID	Secant Stiffness (kN/m)	Ultimate Resistance (kN)
G1 100 400 XX M	663	11,20
G2* 100 400 XX M	218	7,64
G2 100 400 XX M	547	8,92
G2* 150 400 XX M	195	7,60
G2 150 400 XX M	352	9,96
G3 100 400 XX M	588	13,40
G4 100 600 XX M	881	11,16
G5 100 400 XX M	372	8,28
G6 100 400 XX M	261	12,56
G9 100 400 XX M	2361	35,92

Figure 4 Main experimental results of the monotonic tests of the unsheathed configurations

The openings, specimens G1 and G3, seem not to adversely affect the strength and the stiffness of the wall. They may even improve the performance. Figure 5a) compares the bracing systems (G9, G4, G3 and the G2 100 400 XX configurations). It is apparent that the diagonal straps are by far the most effective bracing system. The figure shows also the good performance in terms of stiffness of the configuration with 600 mm of stud spacing (G4 100 600 XX). Besides, the figure further confirms the important role of the hold-downs, since the curve that identifies the configuration without hold-downs (G2 100 400 XX) is the lowest one. As to the sheathed configurations, Figure 5b) compares all the monotonic responses, highlighting i) the incremental resistance provided by the sheathing ii) the limited influence of the type of sheathing on the lateral response and iii) the limited influence of the type of steel frame or bracing system on the lateral response of the wall.
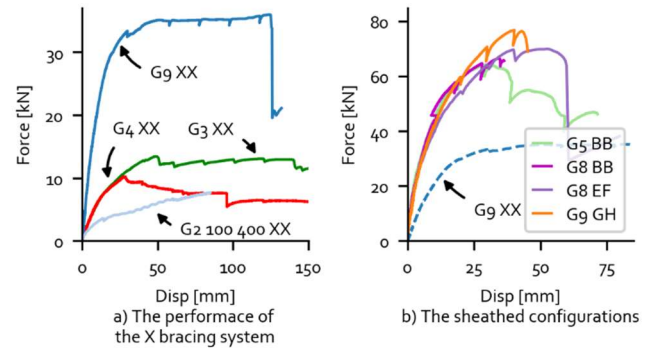

Figure 5 Experimental results of the monotonic tests for unsheathed and sheathed configurations

Table 3   Monotonic test results: sheathed configurations

Specimen ID	Secant Stiffness (kN/m)	Ultimate Resistance (kN)
G5 100 400 BB M	6760	64,20
G7 100 400 AB M	2864	40,40
G8 100 400 BB M	6170	66,48
G8 100 400 EF M	6044	70,04
G9 100 400 GH M	5320	76,92

The cyclic tests enable getting an appraisal of the ductility, the energy dissipation and the cyclic envelope. A total of six cyclic tests were performed, 3 on unsheathed and 3 on sheathed configurations. Three tests are reported in the Figure 6 for one unsheathed and two sheathed configurations. Figure 6a) compares two configurations with the same bracing system demonstrating that the sheathing increases the strength and the stiffness but reduces the ductility.

All cyclic responses highlight the substantial pinching behaviour that characterizes these systems, that is mainly due to the connection behaviour. As shown in Figure 6b), the cyclic response of the G8 100 400 EF configuration exhibits a strength degradation only after 40 mm of displacement, indeed before this limit, the monotonic and cyclic envelopes coincide. This phenomenon can be associated with the damage of the panel-to-member connections since the lateral response of this configuration is mainly governed by the connections response.
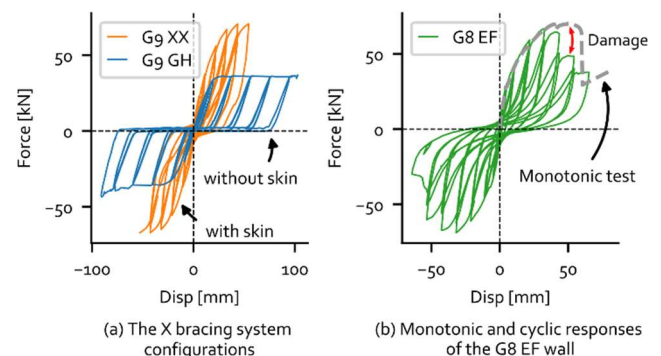

Figure 6 Force-displacements curve for specimens G9 and G8

3   The numerical simulation

The results of the experimental tests have enabled the development

of numerical models based on the finite element method. Among all configurations of the experimental program, 3 of them were selected in order to develop numerical models making particular attention to the sheathed solutions.

As proved in section 2.2, the sheathing is one of the main components that improve the lateral response of the walls, on the other hand, the mechanism of forces transmission between the panels and the steel frame is difficult to be caught. At this aim, two sheathed configurations, representative of the two limit cases, were modelled and analysed: i) the G9 100 400 GH and ii) the G8 100 400 EF. These configurations represent the wall with the best steel bracing system (G9) and the wall with no steel bracing (G8). In addition, to properly simulate the behaviour of the G9 steel frame also the unsheathed G9 wall (G9 100 400 XX) was modelled and analysed. Therefore, a total of 6 tests on 3 configurations were simulated, aiming at understanding the mechanisms of forces transfer between the wall's components (i.e., the steel frame elements and the sheathing). Figure 7 shows the three configurations: i) the G9 100 400 XX (G9 XX) is an unsheathed configuration characterized by diagonal straps with double outer chords, and hold-downs on external chords, ii) the G8 100 400 EF (G8 EF) has no bracing systems but it has the sheathing on both sides and iii) the G9 100 400 GH (G9 GH) configuration has the same steel frame of the G9 XX but has sheathing. The two sheathed and one unsheathed walls, were modelled and analysed using the OpenSees software [14] under monotonic and cyclic loading. All these configurations were analysed using a static approach to simulate both the monotonic and cyclic loading history.
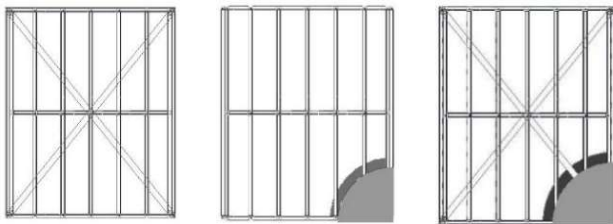
a)   G9 100 400 XX   b)   G8 100 400 EF   c)   G9 100 400 GH
Figure 7 Wall configurations considering in the numerical simulations

The model of the unsheathed wall is created in a 2D space with 3 degrees of freedom, while the models for the sheathed configurations are built in a 2D or 3D space with 3 or 6 degrees of freedom, respectively. This difference is entirely due to the type of method used to simulate the sheathing panels. Since the G9 configurations differ from the G8 for the presence of a diagonal bracing system only, the skeleton of all 3 configurations is modelled in the same way as shown in Figure 8. In detail, 'dispBeamColumn' elements are used to simulate the behaviour of the CFS members. ZeroLength elements (ZLEs) are used to simulate the hold-downs response since these elements have no physical dimension, and a wide range of 'rheological' models of behaviour can be associated to them. This feature makes them suitable to simulate also the connections behaviour, such as the sheathing-to-member connections.

The diagonal straps of the G9 configurations have to transfer only axial forces; they were hence modelled through "truss" elements. Shell elements or rigid constraints, depending on the model dimension (3D or 2D), were used to simulate the panels of the sheathed configurations (G9 GH and G8 EF). The panels are placed on the external faces of the walls, and the sheathing is hence symmetric with respect to the mid-plane of the wall. One single layer was hence used, as shown in Figure 9.
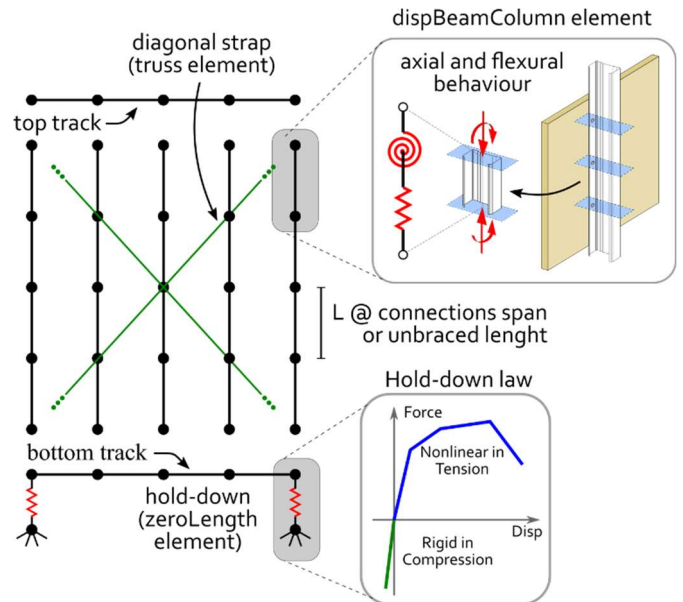

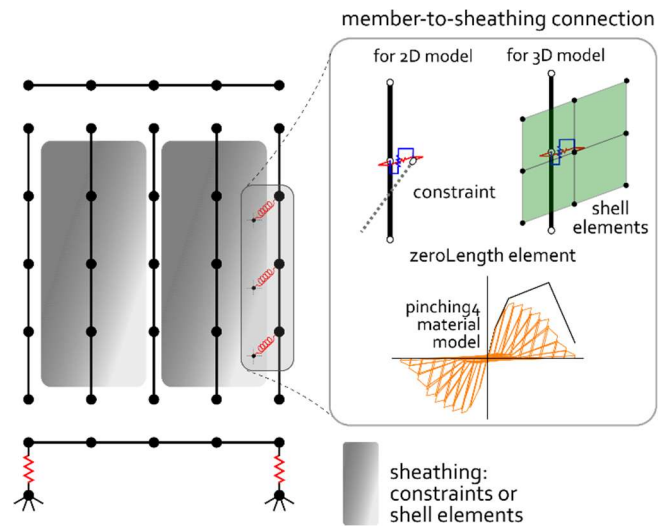**Figure 8** Model details of the steel frame

Figure 9 Model details of the sheathing and its connections to steel skeleton

All the mentioned components significantly affect the global response of the wall, triggering several sources of nonlinearities. For this reason, accurate characterization of all model elements is needed. The complexity of these systems and the partial lack of experimental data suggest the use of a mixed experimental-numerical approach, as in the following.

3.1   The components' characterization

The finite elements, used to simulate the components of the shear walls, were introduced in the previous section but they were not defined in detail. This section focusses on the characterisation of: the axial and bending behaviour of the members, the shear behaviour of the sheathing-to-member connections, the hold-down response and the axial response of the straps.
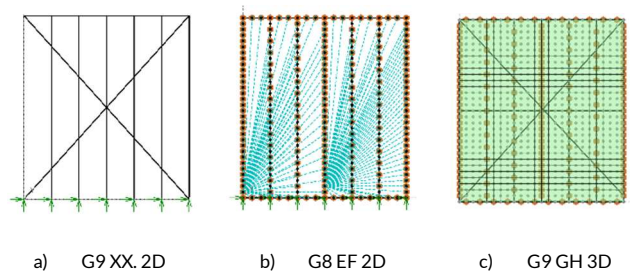
a)   G9 XX. 2D   b)   G8 EF 2D   c)   G9 GH 3D
Figure 10 Numerical models created using OpenSees

3.1.1 Members

The resistance and the stiffness of cold-formed steel members are related to their length, due to the several buckling phenomena that can occur in compression. They need hence a specific characterization accounting for their restraints. The axial and flexural behaviours were characterized using ABAQUS [15] for lengths of 100 mm, 200 mm and 1500 mm. The 100 mm and 200 mm lengths are the connections' spans for the sheathed configurations while, the 1500 mm length, is the unbraced length in the plane of the wall of the members for the unsheathed configuration The models were created using quad shell elements with reduced integration; a fairly fine uniform mesh equal to 5 mm was adopted. With the aim to take into account all the major sources of nonlinearity, the ABAQUS models incorporated both the material and geometrical nonlinearities, the material damage and the member imperfections. In detail:

- The material behaviour was one of the most important parameters to be defined. Young's modulus was set equal to 203.000 MPa while the yielding and the hardening were set according to the experimental tests performed on some coupons. In order to catch the softening behaviour and fracture of the material, the plastic damage according with the work of Bonora [16] was implemented.

- The imperfections were defined through the 1D modal spectral approach developed by Zeinoddini et. al [17]. The 1D modal spectra approach defines the member imperfections through a combination of all the cross-section buckling modes using non constant amplification factors. The amplification factors depend on the coordinate of the longitudinal axis of the member and they are defined through spectra of imperfection that depend on buckling modes. In detail, for each mode the Authors defined a power spectrum of the imperfections that enables generating a random imperfection field as defined in Equation 1

$$f(x, y, z) = \sum_{i=1}^{m=5} \alpha_i(z)\phi_i(x, y) \tag{1}$$

where $\phi_i(x, y)$ is the i-th buckling mode of the cross-section member and $\alpha_i(z)$ the amplification factor defined through an Inverse Fourier transform. The result of this process led to set three different models for each member length and type of action. An example is reported in Figure 11 which show the imperfections generated for a 200 mm member length.
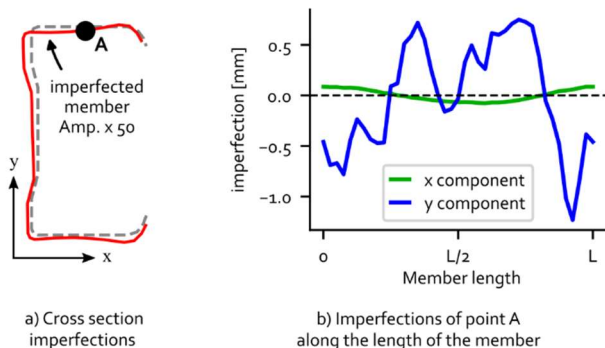

Figure 11 Example of application of the 1D modal spectral approach for the imperfection characterization

All models were then analysed under displacement control using a static approach. In particular, a displacement along the member axis was imposed to characterise the axial behaviour, while rotations of the external sections of members were assumed to characterise the bending behaviour. The results of the analyses were then converted into envelopes and used to define the parameters of the Pinching4 model implemented in OpenSees. Figure 12 shows an example of an ABAQUS simulation for a 200 mm member length subjected to axial load. The mean curve, represented by the black piecewise function, was evaluated averaging the 3 simulations that differ from the imperfection field randomly generated. The averaging process was performed through two steps:

i. each of the 3 curves is converted in a piecewise function with 4 segments according to the Pinching 4 model so that the peak-strength coincides with the second point (Pt. 2), and the dissipated energy is conserved,

ii. the mean curve is then obtained averaging the initial stiffness, the peak-strength and the dissipated energy of the three piecewise functions.
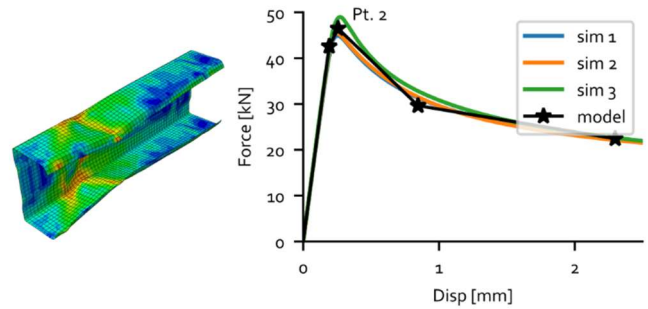

Figure 12 Example of a numerical simulations

Since these results were used as parameters of the Pinching4 material model all the quantities were converted into force-deformation and moment-curvature for axial and flexural behaviour, respectively. These material models were incorporated into the "dispBeamColumn" elements through the section aggregator command that allows the user to combine the models of axial and bending behaviour into the element. It is worth pointing out that even if this procedure is rather accurate, it considers the axial and bending behaviour uncoupled. However, this is of no great importance since the members inside the wall are mainly subjected to axial forces rather than bending.

3.1.2 Diagonal straps

The high slenderness of the diagonal straps makes them subjected to global buckling phenomena. Therefore, they possess negligible stiffness and resistance in compression as confirmed by the experimental tests. Moreover, the straps govern the lateral response of the G9 XX configuration. The stress-strain relation of the material would hence need a proper characterization suitably taking into account the hardening as observed in the coupon tensile test. The Figure 13a) shows the calibration of the steel material model against the experimental data.
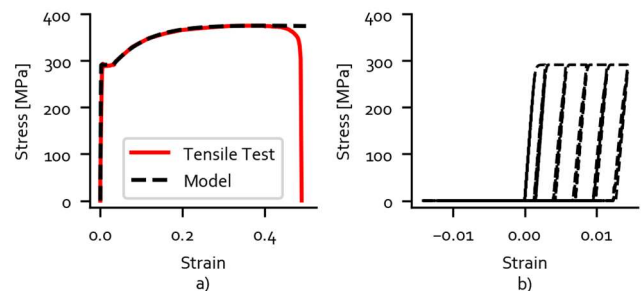

Figure 13 Calibration of the diagonal truss behaviour

With the aim to combine these two aspects, the buckling and the

plasticity, into a single truss element a sort of "trick" was adopted. In detail, the material associated with the truss elements is a series combination of a steel material model (Reinforcing Steel material in OpenSees) and an elastic material with infinite stiffness in tension and no stiffness in compression. This combination enables transferring only the tension forces developed by the trusses as proved by Figure 13b) that shows a cycle test of the combined series material. Indeed, the curve does not exhibit resistance in the compression side.

3.1.3 Hold-downs

The hold-downs have a non-negligible influence on the lateral response of the walls as proved by the experimental tests (Figure 4a)). In particular, both the strength and the stiffness benefit from the presence of the hold-downs. For this reason, an accurate modelling of these components is required to simulate the lateral wall response. At this aim, two ZLEs were placed at the ends of the bottoms track connecting them to the fixed nodes representing the soil as illustrated in Figure 8. The elements are characterized by a rigid behaviour in compression and a nonlinear behaviour in tension. In particular, the tensile behaviour is calibrated through experimental data of hold-down tensile tests [11,12] as shown in Figure 14. The fitting of the experimental data preserves the initial stiffness and the energy dissipated up to peak point (Pt. 3 in Figure 14).
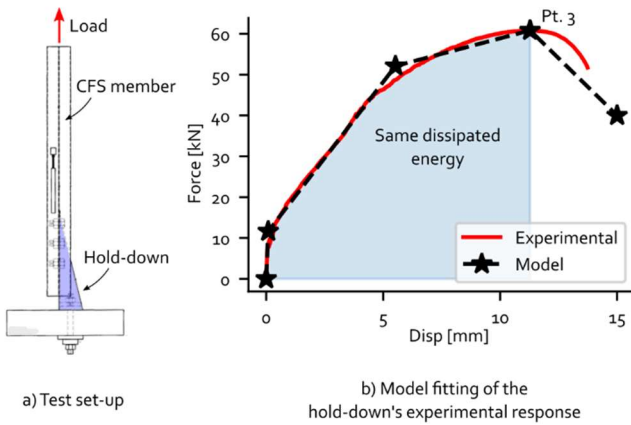

Figure 14 Model fitting of the hold-down's experimental response

3.1.4 Sheathing

The sheathing, characterized by two panels per side, was approximated with a single layer laid in the mid-plane of the shear-wall. The layer has the two panels, modelled through either elastic shell elements or beam constraints for 3D and 2D models, respectively (Figure 15). The 3D model has a uniform mesh of 100 mm in order to allow matching the connections pattern (Figure 10c). The elements are elastic shell elements with an elastic modulus of 33000 MPa according to the product specifications, and they have a thickness equal to twice the actual thickness of the panels since the layers have to simulate both sides of the walls. The elements do not take into account the material nonlinearities given that all deformations are localized into the connections. On the contrary, the constraints applied to the 2D models, were defined by means of rigid links that bound all nodes of the panels. In this case, the nodes are located only in the connection points thereby leading to a reduction of the number of nodes (Figure 15b)). This procedure enables simulation of the panels' behaviour as a sort of a rigid diaphragm. These two different solutions allow investigating on the influence of the sheathing deformability on the wall response since the 2D model exhibits a rigid behaviour of the panels while the 3D model considers an elastic behaviour of these ones. The error due to the assumption of rigid sheathing can be appraised comparing the results of these two solutions.
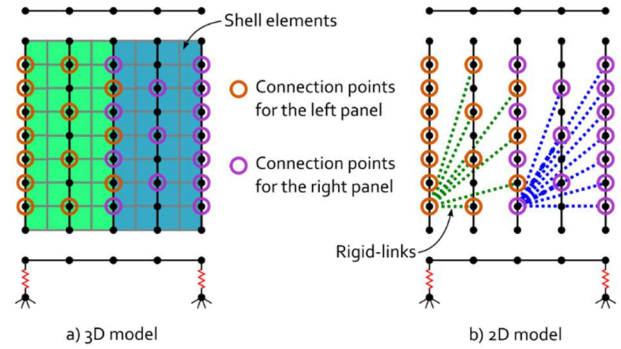

Figure 15 Sheathing model used in the sheathed configurations

3.1.5 Sheathing-to-member connections

The sheathing-to-member connections are the components that govern the stiffness and the resistance of the sheathed configurations, as confirmed by the experimental tests that showed a concentration of the deformations in these points. For this reason, these connections need an adequate characterization considering both monotonic and cyclic behaviour.
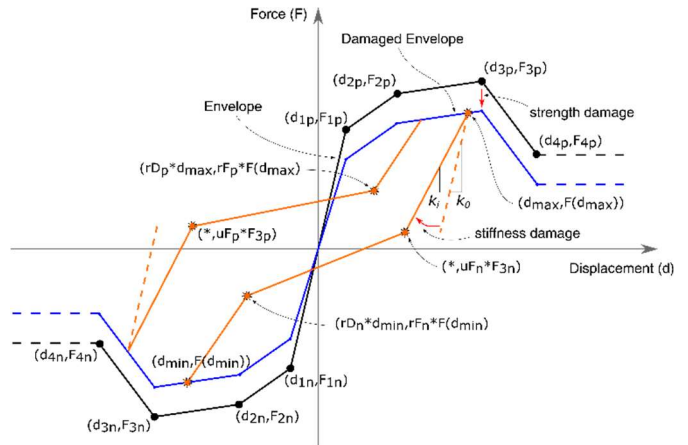

Figure 16 Definition of the Pinching4 Material model implemented in OpenSees

At this aim, the sheathings-to-member connections are modelled through ZLEs to which the "Pinchig4 material" models in Figure 16 are assigned. These rheological models are very useful to simulate cyclic responses that show pinching behaviour and damage typical of these connections. Moreover, the connections have to take into account the fact that the two sides of the wall are combined in a single one since the sheathing was modelled only by one layer. Therefore, the rheological model assigned to the ZLEs of the connections has to be a parallel combination of the two different material models that simulate the single member-to-panel connection. The work of Tao at al. [18] provided the base to define the parameters of the Pinching4 material model. In particular, the Authors provide values for the envelope and pinching parameters depending on the type of connections. Moreover, the values of the parameters depend on both the type of sheathing and the type of analysis: monotonic or cyclic. The Pinching4 model of the connection behaviour of the G8 EF configuration, required incorporation of the strength damage in order to catch the degradation of the cyclic wall response, observed after the peak-strength (Figure 6b)).

3.2 The analyses and the simulation results

The models were analysed through a static analysis under displacement control. The constraints were enforced either by the plain method (Plain Constraint) or by the Lagrange multiplier method. The plain method is used in the 3D model and in the 2D models without sheathing given that the models are characterized by equal DOF

constraints. The Lagrange method is used in the 2D models with sheathing because of beam constraints generate a non-identity constraint matrix. Since the model contains various nonlinearities the solution algorithm was embedded in a convergence algorithm that would adjust the displacement increment and would change the solution algorithm if the current one fails. In Figure 17 the results of the monotonic analyses of the G9 XX, G9 GH and G8 EF models are shown and compared with the experimental curves. All numerical curves are in good accordance with the experimental ones in terms of both stiffness and strength. Besides, Figure 17b) shows a limited difference between the monotonic analysis of the 2D and 3D models of the G9 GH wall confirming that the 2D model can be adopted given the lower time of the analysis.
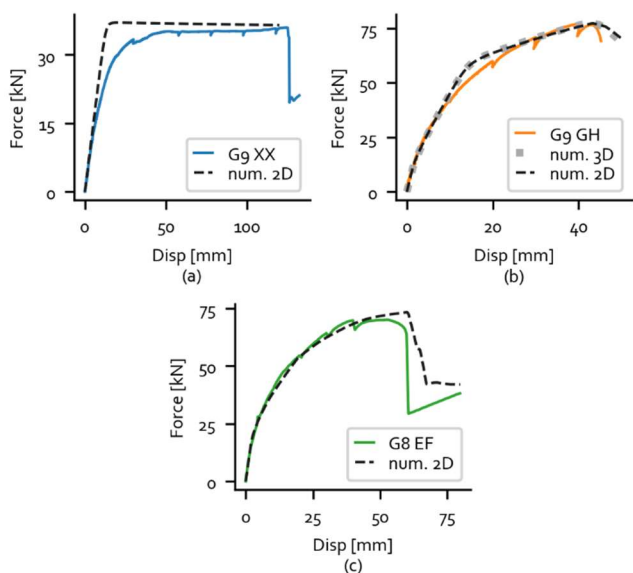

Figure 17 Results of the monotonic analyses

For the sheathed configuration Figure 18a) and Figure 18b) show the reaction forces of the sheathing-to-members connections at the maximum strength point. Each panel is identified by a different colour and the stress level can be evaluated by the arrow's length. As expected, the more stressed elements are the ones at the corners of the panels and in the mid seams between two panels. This is proved by Figure 19 and Figure 20 that show how the vertical and horizontal components of the connectors forces are distributed.
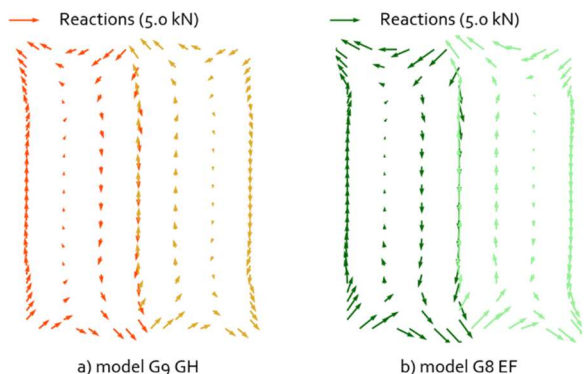

Figure 18 Connection reactions at the maximum strength of the monotonic response

The cyclic analyses were performed only for the 2D models since they are less time consuming, and their accuracy is practically the same of the 3D shell models as proved by the monotonic analyses. The loading protocol adopted in the three cyclic simulations is the same of the one used in the experimental tests in order to make the results comparable. At this aim, the results of the cyclic simulations

are reported in Figure 21, which compares the numerical and experimental response in terms of force-displacement curves. All the models provided very good approximations in terms of both stiffness and resistance. Moreover, they were able to reproduce the pinching effect typical of these systems.
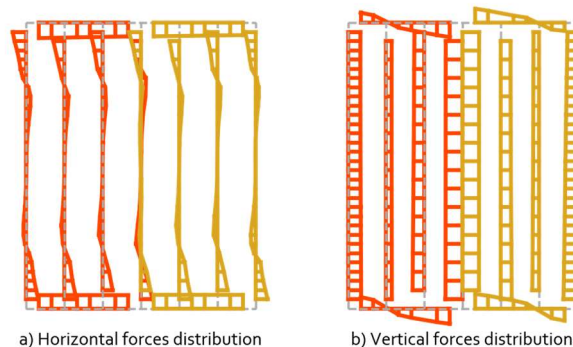

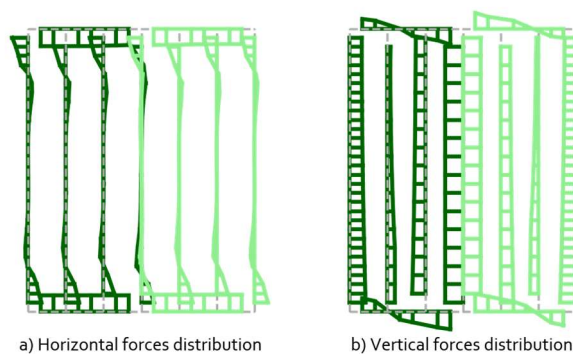**Figure 19** Distribution of the horizontal and vertical components of the connections forces of G9 GH model

Figure 20 Distribution of the horizontal and vertical components of the connections forces of G8 EF model
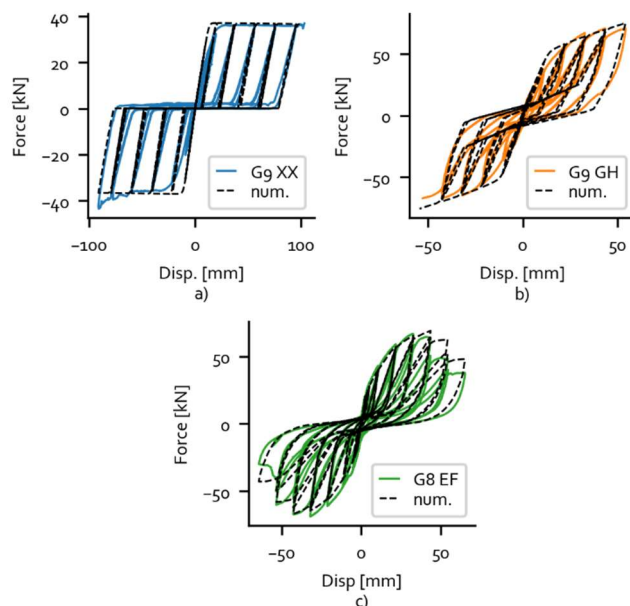

Figure 21 Results of the cyclic analyses

The dissipated energy can be used as an effective parameter to assess the accuracy of the numerical solution. Therefore, Figure 22a) shows the energy dissipated during the analyses while Figure 22b) shows the energy dissipated cycle by cycle. All the results show a good approximation of the experimental tests for the sheathed con-

figurations with a small overestimation of the energy in the last cycles. On the contrary, the unsheathed model of configuration G9 XX, tends to underestimate the energy in the last cycles. This is mainly due to the high pinching effect that the model exhibits.
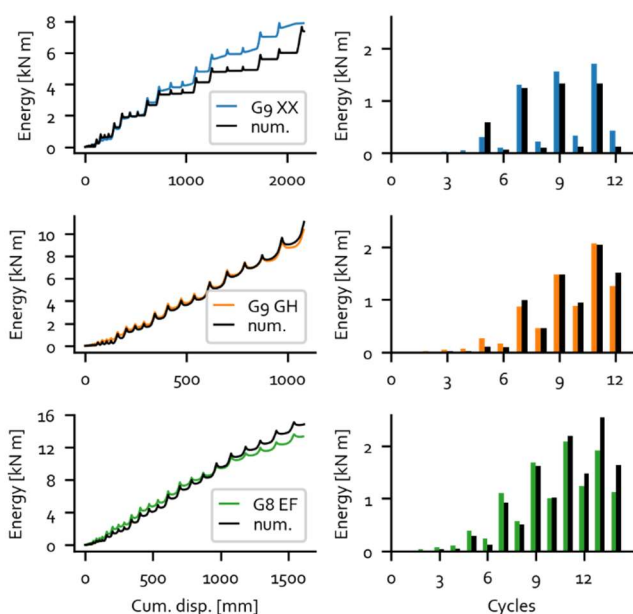

Figure 22 Energy dissipated during the cyclic analyses

It is worth pointing out that the pinching effect has different sources depending on the type of wall configuration. Indeed, the pinching developed by the unsheathed configuration (G9 XX) is only due to the buckling effect of the compressed diagonal straps. On the other side, the pinching observed in the sheathed configurations (G9 GH and G8 EF) is due to the cyclic behaviour of the connections, as proved by the Figure 23a) that shows a connections response of the G8 EF model during the analysis.
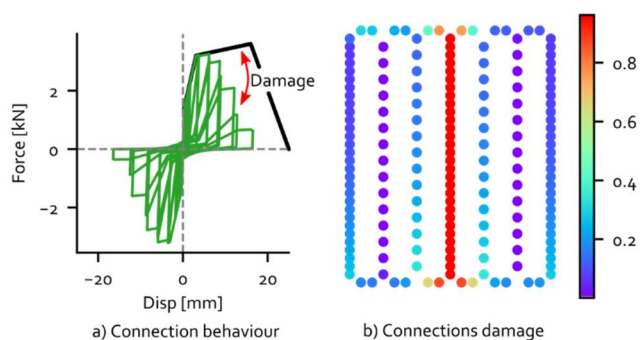

Figure 23 Connections response and damage of the G8 EF model.

As already mentioned, the damage was embedded in the connection model used in the G8 EF configuration. This feature enables a better simulation of the latest cycles of the wall response characterized by a wall strength reduction. In detail, Figure 23a) shows the effect of the damage in the connection behaviour while Figure 23b) shows the level of the damage of the connections at the end of the analysis. The connection placed at the mid seam between two panels resulted the more damaged consistently with the forces distribution reported in Figure 18.

4 Conclusions

The study presented herein focussed on the shear behaviour of the shear walls used in light residential steel buildings. At this aim, an ex-

perimental and numerical analysis was performed. The paper summarizes the experimental program, highlighting the main features and constructional details that govern the lateral response of the walls. The experimental results enabled the development of numerical models with the aim to understand the mechanism of the forces transfer in these systems and extend the cases of study. Therefore, three numerical models are then developed and analysed using OpenSees software: one without sheathing (G9 XX) and two with sheathing (G9 GH and G8 EF). The models consider all the main sources of nonlinearity such as the axial and bending behaviour of the members, the buckling and plastic behaviour of the diagonal straps and the connections responses. The members were simulated through beam-column elements whose behaviour was characterised through ABAQUS simulations. With this approach, a simple FE, such as beam-column element, can simulate the member response taking into account the imperfections, the material properties and the post-buckling behaviour. Particular care was taken to model the connections since they considerably affect the global response of the sheathed configurations, affecting the pinching behaviour exhibited under cyclic loading. Eventually, the agreement between the numerical and the experimental responses in terms of initial stiffness, strength and dissipated energy is more than satisfactory, validating the approach.

References

[1] Al-Kharat, M.; Rogers, C.A. (2007) *Inelastic performance of cold-formed steel strap braced walls.* Journal of Constructional Steel Research **63**, 460–474.

[2] Al-Kharat, M.; Rogers, C.A. (2008) *Inelastic performance of screw-connected cold-formed steel strap-braced walls.* Canadian Journal of Civil Engineering, **35**(1), 11-26.

[3] DaBreo, J.; Balh, N.; Ong-Tone, C.; Rogers, C.A. (2014) *Steel sheathed cold-formed steel framed shear walls subjected to lateral and gravity loading.* Thin-Walled Structures **74**, 232-245.

[4] Buonopane, S.G.; Bian, G.; Tun, T.H.; Schafer, B.W. (2015) *Computationally efficient fastener-based models of cold-formed steel shear walls with wood sheathing.* Journal of Constructional Steel Research **110**, 137–148.

[5] Liu, P.; Peterman, K.D.; Schafer, B.W. (2012) *Test Report on Cold-Formed Steel Shear Walls.* Research report CFS-NEES–RR03. Buffalo, USA: SUNY.

[6] Lu, S. (2015) *Influence of gypsum panels on the response of cold-formed steel framed shear walls,* Doctoral thesis. Montreal, CND: Mc Gill University.

[7] Chen, C.Y. (2004) *Testing and performance of steel frame/wood panel shear walls,* Doctoral thesis. Montreal, CND: Mc Gill University.

[8] Padilla-Llano, D.; Ding, C.; Moen, C.D. (2015) *Advancing Seismic Simulation of Cold-Formed Steel Framed Buildings,* Report No. CE/VPI-ST-15/05. Blacksburg, VA: Virginia Tech.

[9] Schafer, B.W.; Ayhan, D.; Leng, J.; Liu, P.; Padilla-Llano, D.; Peterman, D.; Stehman, M.; Buonopane, S.G.; Eatherton, M.; Madsen, R.; Manley, B.; Moen, C.D.; Nakata, N.; Rogers, C.A.; Yu, C.

(2016) *Seismic response and engineering of cold-formed steel framed buildings*. Structures **8**(2), 197-212.

[10] ECCS (1986) *Recommended Testing Procedure for Assessing the Behaviour of Structural Steel Elements under Cyclic Loads*, Publication P045, Brussels: European Convention for Constructional Steelworks.

[11] University of Trento (2014), *SteelMax: experimental and numerical analysis of the performance of CFS profiles and subassemblies under elementary and complex states of stress*, Research report. Trento: Department of Civil, Environmental and Mechanical Engineering (in Italian).

[12] Accorti, M.; Baldassino, N.; Zandonini, R.; Scavazza, F.; Rogers, C.A. (2016) *Response of CFS Sheathed Shear Walls*. Structures **7**, 100-112.

[13] AISI S907-2013 (2013) *Test Standard for Cantilever Test Method for Cold-Formed Steel Diaphragms* – Washington DC, USA: American Iron and steel Institute.

[14] OpenSees Command language Manual, http://opensees.berkeley.edu/wiki/index.php/Command_Manual

[15] Abaqus (2016) Online Documentation, http://50.16.225.63/v2016/

[16] Bonora, N. (1997) *A non linear CDM model for ductile failure*. Engineering Fracture Mechanics **58**, I/2, 11-28.

[17] Zeinoddini, V.M.; Schafer, B.W. (2012) *Simulation of Geometric Imperfections in Cold-Formed Steel Members Using Spectral Representation Approach*. Thin-Walled Structures **60**, 105–117.

[18] Tao, F.; Chatterjee, A.; Moen, C.D. (2016) *Monotonic and Cyclic Response of Single Shear CF Steel-to-Steel and Sheathing-to-Steel Connections*, Report No. CE/VPI-ST-16-01, Blacksburg, VA: Virginia Tech.